



## A new series of Cs<sup>+</sup>, K<sup>+</sup> and Na<sup>+</sup> chelators: Synthesis, kinetics, thermodynamics and modeling

Alexandre Korovitch<sup>a</sup>, Antoine Le Roux<sup>b</sup>, Florent Barbault<sup>a</sup>, Miryana Hémadi<sup>a</sup>,  
 Nguyêt-Thanh Ha-Duong<sup>a</sup>, Claude Lion<sup>a</sup>, Alain Wagner<sup>b</sup>, Jean-Michel El Hage Chahine<sup>a,\*</sup>

<sup>a</sup> Université Paris Diderot Sorbonne Paris Cité – CNRS, Interfaces, Traitements, Organisation et Dynamique des Systèmes, UMR 7086, Bâtiment Lavoisier, 15 Rue Jean-Antoine de Baïf, 75205 Paris Cedex 13, France

<sup>b</sup> Laboratoire des Systèmes Chimiques Fonctionnels, UMR 7199, Faculté de Pharmacie, 74 Route du Rhin, BP 24, 67401 Illkirch-Graffenstaden, France

### ARTICLE INFO

#### Article history:

Received 19 June 2012

Accepted 5 August 2012

Available online 29 August 2012

#### Keywords:

Radioactive decontamination

Norbadione

Relaxation kinetics

Complex formation

Stopped-flow

Mechanism

### ABSTRACT

The synthesis of two molecules, B1 and B2, based on elements of norbadione A, the natural Cs<sup>+</sup> chelator in mushrooms, associated, in the case of B2, with an 18-crown-6 ether is reported. Thermodynamic and kinetic analyses performed in water, ethanol and ethanol/water 9/1 v/v (M1) show in M1 and ethanol that B1 and B2 form stable complexes with Na<sup>+</sup>, K<sup>+</sup> and Cs<sup>+</sup>. Affinity constants, measured spectrophotometrically in ethanol and M1, by the use of the SPECTFIT program, are in the 10<sup>5</sup> and 10<sup>6</sup> range for B1 and B2, respectively. The second-order rate constants are in the 10<sup>6</sup>–10<sup>7</sup> M<sup>-1</sup> s<sup>-1</sup> range and the first-order rate constants about unity. The ratios of the second-order/first-order rate constants confirm the thermodynamic results in EtOH. The kinetic processes become much too fast to allow runs in M1. Molecular simulations in EtOH imply the existence of two isomers for each of the Cs<sup>+</sup>/B1 and Cs<sup>+</sup>/B2 complexes. With B1, the more stable one is that in which the two enolates are parallel and mimic the alkali-metal inclusion cavity already envisaged for norbadione A. With B2, two similar structures are extracted, in both of which Cs<sup>+</sup> is included in the crown ether and capped by the enolate. The affinity of B1 for Cs<sup>+</sup> is comparable to that of norbadione A, whereas that of B2 is higher. These results are encouraging as they introduce a new series of alkali chelators which can lead to molecules capable of complexing <sup>137</sup>Cs<sup>+</sup> for radioactive decontamination.

© 2012 Elsevier B.V. All rights reserved.

### 1. Introduction

Alkali metals, such as sodium and potassium, are absolutely essential for life, whereas others, such as cesium or lithium, are not required for biological processes. However, despite this fact, up to 1.5 mg of cesium is present in the human body [1]. Its stable isotope, <sup>133</sup>Cs is considered innocuous or slightly toxic because of its interference with sodium potassium pump [2,3]. Nonetheless, 38 other radioactive isotopes, such as <sup>135</sup>Cs and <sup>137</sup>Cs, are generated during nuclear reactions. The most dangerous to health is <sup>137</sup>Cs with a half-life of 30 years. <sup>137</sup>Cs is produced in nuclear power plants by the chain decay of <sup>235</sup>U to <sup>137</sup>Te and then <sup>137</sup>Cs [4]. During the Chernobyl disaster in 1986 and very recently during that of Fukushima, large amounts of <sup>137</sup>Cs were released [5–8]. It should also be noted that more than 20 million people live within a range of 30 km of a nuclear power plant. This renders <sup>137</sup>Cs accumulation a potential major health problem [7–9]. In Europe, after Chernobyl, <sup>137</sup>Cs was partly accumulated in norbadione A (NbA), the essential pigment of the bay boletus mushroom [10–13]. NbA is a naphtholactone

related to a family of mushroom pigments, the pulvinic acids (Fig. 1) [10,14].

Complex formations of alkali metals are considered to be extremely fast processes, which are practically diffusion-controlled [15–17]. However, with some sterically hindered and capped calix[4–8]arenes, or with NbA, they can be slow to very slow [18–20]. Most of the other investigations concerning these complexes were performed by <sup>1</sup>H, <sup>13</sup>C and/or <sup>133</sup>Cs NMR. They always indicated fast kinetic processes occurring in the sub-second time range [21]. These are also assumed to be host–guest processes that occur with crown ethers and with calixarenes [22–26]. On the other hand, apart from NbA, alkali metal complexes with classical chelators, that do not have an inclusion cavity, are quite rare [10,11,16,18,27]. Furthermore, the elementary tetronic and pulvinic acid building blocks that constitute NbA do not complex alkali metals (Fig. 1) [18]. Complex formation occurs because of the particular structure of NbA [18,28]. The aim of this work is to mimic NbA in complex formation with alkali metals by synthesizing a structure based on tetronic acid, to associate a tetronic acid with crown ether, and to analyze by means of chemical relaxation, fast kinetics and molecular simulation the mechanisms involved in complex formation with Na<sup>+</sup>, K<sup>+</sup> and Cs<sup>+</sup>.

\* Corresponding author. Tel.: +33 157277238; fax: +33 157277263.

E-mail address: [chahine@univ-paris-diderot.fr](mailto:chahine@univ-paris-diderot.fr) (J.-M. El Hage Chahine).

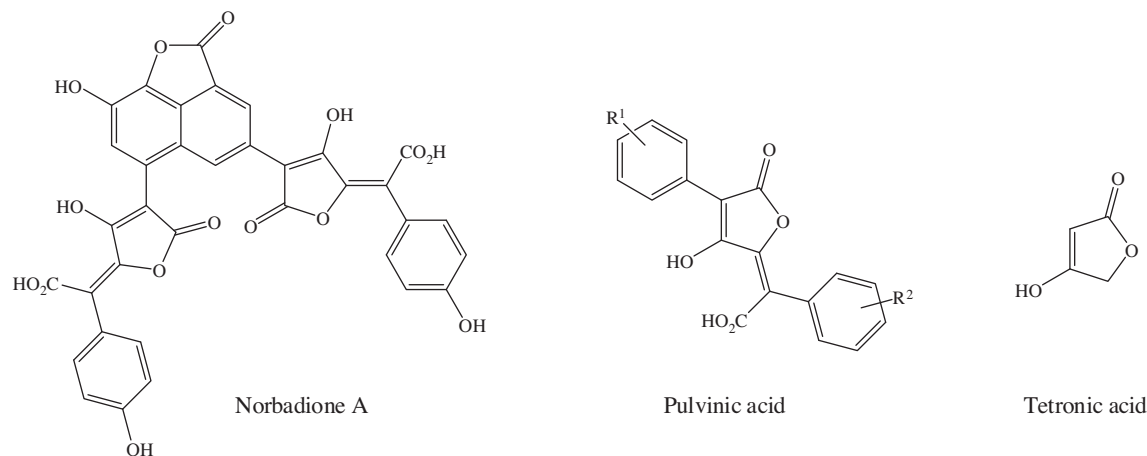


Fig. 1. Molecular structures of norbadione A and its components; pulvinic and tetrone acids.

## 2. Experimental

### 2.1. Synthesis

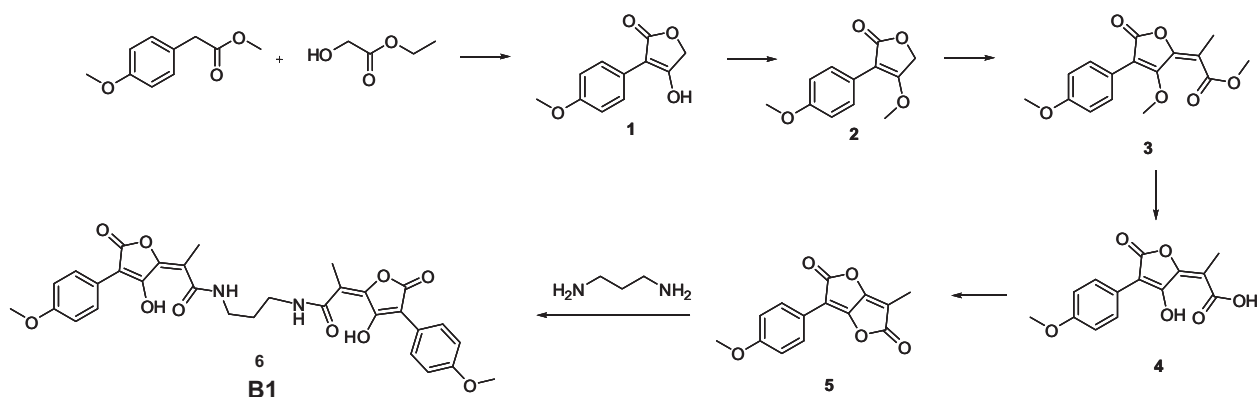
Commercial reagents were used without further purification. Anhydrous tetrahydrofuran (THF) was obtained by distillation over sodium and benzophenone. Analytical thin layer chromatography (TLC) was performed using plates cut from glass sheets (silica gel 60F-254 from Merck). Detection was performed under a 254 or 365 nm UV light and by immersion in an ethanol solution of cerium sulfate, followed by heating. Compounds were purified on a Silica gel 60 chromatography column. IR spectra were recorded in CH<sub>2</sub>Cl<sub>2</sub> solutions or in the solid state on a diamond plate on a Nicolet 380 FT-IR spectrometer from Thermo Electron Corporation. <sup>1</sup>H and <sup>13</sup>C NMR spectra were recorded at 23 °C on a Bruker 400 MHz, Bruker 300 MHz or Bruker 200 MHz spectrometers. Recorded shifts are reported in parts per million (δ) and calibrated with residual undeuterated solvent. Data were represented as follows: Chemical shift, multiplicity (s = singlet, d = doublet, t = triplet, m = multiplet), integration and coupling constant (J, Hz). High resolution mass spectra (HRMS) were obtained using an Agilent Q-TOF (time of flight) 6520 instrument and low resolution mass spectra using an Agilent MSD 1200 SL. Electrospray ionization/atmospheric pressure chemical ionization (ESI/APCI) was performed on an Agilent HPLC1200 SL.

#### 2.1.1. 4-Hydroxy-3-(4-methoxyphenyl)-furan-2(5H)-one (**1**)

Ethyl glycolate (2.9 g, 28 mmol, 1 eq) and potassium *tert*-butoxide (6.3 g, 56 mmol, 2 eq) were added to a solution of methyl 4-methoxyphenylacetate (5 g, 28 mmol, 1 eq) in THF (180 mL) and the mixture was refluxed overnight. After cooling to room temperature, concentrated HCl was added until acidic and the mixture extracted with ethyl acetate (3 × 100 mL). The combined organic phases were dried over magnesium sulfate and concentrated *in vacuo*. Crystals formed during the evaporation process were collected and washed with diethyl ether. The filtrate was concentrated, and the operation repeated until the end of precipitation. Yield: 78%; <sup>1</sup>H NMR (300 MHz, DMSO-*d*<sub>6</sub>): δ = 3.75 (s, 3H), 4.74 (s, 3H), 6.94 (d, 2H, *J* = 9.0 Hz), 7.84 (d, 2H, *J* = 9.0 Hz), 12.58 (s, 1H); <sup>13</sup>C NMR (DMSO-*d*<sub>6</sub>): δ = 55.0, 66.0, 97.3, 113.5, 122.9, 127.6, 157.6, 173.1, 173.3; MS (ESI) *m/z* 207.1 ([M+H]<sup>+</sup>).

#### 2.1.2. 4-Methoxy-3-(4-methoxyphenyl)-furan-2(5H)-one (**2**)

Potassium carbonate (2.8 g, 20 mmol, 1 eq) and dimethyl sulfate (2.5 g, 20 mmol, 1 eq) were added to a suspension of **1** (4.1 g, 20 mmol, 1 eq) in acetone (85 mL), and the suspension refluxed for 4 h. After cooling to room temperature, the solid was filtered off over Celite. The filtrate was concentrated to give **2** as a white solid and which was used for the next step without further purification. Yield: 99%; <sup>1</sup>H NMR (200 MHz, CDCl<sub>3</sub>): δ = 3.76 (s, 3H), 3.86 (s, 3H), 4.72 (s, 2H), 6.86 (d, 2H, *J* = 8.8 Hz), 7.77 (d, 2H, *J* = 8.8 Hz);



$^{13}\text{C}$  NMR ( $\text{CDCl}_3$ ):  $\delta = 55.3, 58.0, 64.6, 102.1, 113.7, 121.9, 128.9, 158.9, 172.3, 173.1$ ; MS (ESI)  $m/z$  221.1 ( $[\text{M}+\text{H}]^+$ ).

### 2.1.3. Methyl 2-(3-methoxy-4-(4-methoxyphenyl)-5-oxofuran-2(5H)-ylidene)-propanoate (**3**)

A solution of diisopropylamine (4.2 mL, 30 mmol, 1.5 eq) in anhydrous THF (125 mL) was cooled to  $-20^\circ\text{C}$ , and then  $n\text{BuLi}$  (1.6 M solution, 18.7 mL, 30 mmol, 1.5 eq) was added dropwise. The mixture was stirred for 30 min and afterwards cooled to  $-78^\circ\text{C}$ . A solution of **2** (4.4 g, 20 mmol, 1 eq) in anhydrous THF (65 mL) was added dropwise and the mixture was stirred for 30 min before dropwise addition of methyl pyruvate (6.1 mL, 60 mmol, 3 eq). The mixture was stirred for 30 min at  $-78^\circ\text{C}$  and then warmed to room temperature. A saturated solution of ammonium chloride was added, the aqueous layer extracted with ethyl acetate ( $3 \times 60$  mL), and the combined organic phases dried over magnesium sulfate and concentrated *in vacuo*. The resulting oil was diluted in dichloromethane (DCM, 200 mL) and cooled to  $0^\circ\text{C}$ . Triethylamine (16.7 mL, 120 mmol, 6 eq), 4-dimethylamino-pyridine (240 mg, 2 mmol, 0.1 eq) and trifluoroacetic anhydride (1.26 g, 60 mmol, 3 eq) were added dropwise, successively. The mixture was stirred overnight at room temperature and then acidified by 1 M HCl. The aqueous phase was extracted with DCM, ( $3 \times 50$  mL), and the combined organic phases dried over magnesium sulfate and concentrated *in vacuo*. The crude was then purified by chromatography (cyclohexane/ethyl acetate 90/10 to 50/50) to give **3** as a mixture of *E* and *Z* ( $E/Z = 70/30$ ). Yield: 88%;  $^1\text{H}$  NMR (300 MHz,  $\text{CDCl}_3$ ): isomer *E*:  $\delta = 2.15$  (s, 3H), 3.72 (s, 3H), 3.82 (s, 3H), 3.83 (s, 3H), 6.92–6.95 (m, 2H), 7.41–7.43 (m, 2H); isomer *Z*:  $\delta = 2.27$  (s, 3H), 3.80 (s, 3H), 3.83 (s, 3H), 3.86 (s, 3H), 6.93–6.96 (m, 2H), 7.40–7.43 (m, 2H);  $^{13}\text{C}$  NMR ( $\text{CDCl}_3$ ): isomer *E*:  $\delta = 15.2, 52.8, 55.6, 61.1, 109.0, 113.4, 114.2, 120.8, 131.4, 143.3, 160.3, 161.3, 168.2, 168.7$ ; MS (ESI)  $m/z$  305.1 ( $[\text{M}+\text{H}]^+$ ).

### 2.1.4. 2-(3-Hydroxy-4-(4-methoxyphenyl)-5-oxofuran-2(5H)-ylidene)-propanoic acid (**4**)

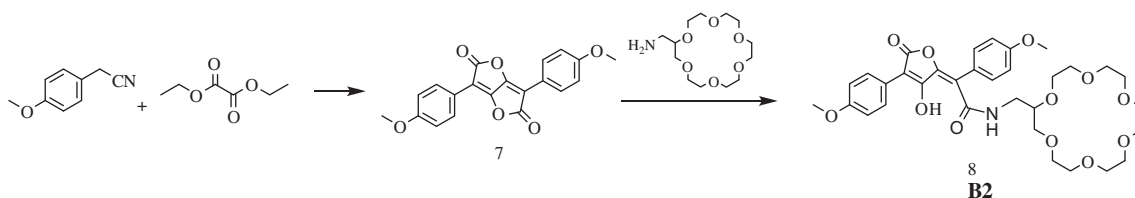
Magnesium bromide (184 mg, 1 mmol, 1 eq) was added to a solution of **3** (304 mg, 1 mmol, 1 eq) in dimethylformamide (DMF) (10 mL) and the mixture stirred at  $120^\circ\text{C}$  until no more starting material remained. The solvent was removed under reduced pressure, and the crude diluted in water. The organic phase was washed with dichloromethane ( $3 \times 15$  mL), and acidified with 1 M HCl. The aqueous phase was extracted with ethylacetate ( $3 \times 15$  mL). The combined organic phases were washed with brine, dried over sodium sulfate and concentrated to give **4**. Yield: 78%;  $^1\text{H}$  NMR (200 MHz, MeOD):  $\delta = 2.11$  (s, 3H), 3.81 (s, 3H), 6.92 (d, 2H,  $J = 9.0$  Hz), 8.02 (d, 2H,  $J = 9.0$  Hz);  $^{13}\text{C}$  NMR:  $\delta = 14.5, 55.6, 103.9, 114.1, 114.6, 123.4, 129.9, 154.6, 160.6, 160.9, 168.3, 174.7$ ; MS (ESI)  $m/z$  231.0 ( $[\text{M}-\text{CO}_2]^-$ ).

### 2.1.5. 3-(4-Methoxyphenyl)-6-methylfuro[3,2-b]furan-2,5-dione (**5**) [29,30]

**4** (1 g, 3.6 mmol) was suspended in acetic anhydride (17 mL), heated to reflux for 1 h and then cooled to room temperature. During cooling, yellow crystals appeared which were collected by filtration and washed with pentane to give **5**. Yield: 94%;  $^1\text{H}$  NMR (300 MHz,  $\text{CDCl}_3$ ):  $\delta = 2.06$  (s, 3H); 3.86 (s, 3H); 6.98 (d, 2H,  $J = 9.1$  Hz); 7.94 (d, 2H,  $J = 9.1$  Hz); 2.06 (s, 3H); 3.86 (s, 3H); 6.98 (d, 2H,  $J = 9.1$  Hz); 7.94 (d, 2H,  $J = 9.1$  Hz);  $^{13}\text{C}$  NMR ( $\text{CDCl}_3$ ):  $\delta = 7.64, 55.5, 98.8, 101.1, 114.8, 119.0, 129.9, 155.6, 159.3, 161.0, 166.1, 168.8$ ; MS [ESI + APCI]  $m/z$  258.0 ( $\text{M}^+$ ).

### 2.1.6. (2*E*,2'*E*)-*N,N'*-(Propane-1,3-diyl)bis(2-(3-hydroxy-4-(4-methoxyphenyl)-5-oxofuran-2(5H)-ylidene) propanamide) (**6**) [31]

A suspension of **5** (200 mg, 0.77 mmol, 1 eq) in anhydrous THF (15 mL) was cooled to  $-35^\circ\text{C}$ , before adding a solution of tetra-*N*-butylammonium fluoride (TBAF) (1.0 M in THF, 1.55 mL, 1.55 mmol, 2 eq). The mixture was stirred for 15 min and then cooled to  $-78^\circ\text{C}$ . A solution of 1,3-diaminopropane (33  $\mu\text{L}$ , 0.39 mmol, 0.5 eq) in 5 mL THF was added dropwise and the mixture stirred for 15 min. At room temperature, ethyl acetate was added and the organic phase washed with 1 M HCl and brine, dried over  $\text{MgSO}_4$ , filtered and concentrated. The yellow residue was washed with diethyl-ether and compound **6** collected as a yellow solid. Yield: 57%.  $^1\text{H}$  NMR (pyridine- $d_5$ ):  $\delta = 1.97$  (t, 2H,  $J = 6.8$  Hz), 2.20 (s, 6H), 3.56 (t, 4H,  $J = 6.8$  Hz), 3.67 (s, 6H), 7.10 (d, 4H,  $J = 8.9$  Hz), 8.57 (d, 4H,  $J = 8.9$  Hz);  $^{13}\text{C}$  NMR:  $\delta = 14.4, 29.5, 38.8, 55.6, 101.9, 113.6, 114.7, 124.6, 129.4, 153.1, 159.6, 163.6, 168.3, 170.2$ ; HRMS (ESI): *Anal.* Calc. for  $\text{C}_{31}\text{H}_{31}\text{N}_2\text{O}_{10}$  ( $[\text{M}+\text{H}]^+$ ): 591.19732. Found: 591.1991%; IR: ( $\text{cm}^{-1}$ ): 464, 499, 515, 555, 582, 634, 655, 698, 743, 792, 811, 833, 912, 1027, 1088, 1117, 1151, 1177, 1247, 1295, 1417, 1455, 1485, 1507, 1557, 1602, 1619, 1660, 1739, 2836, 2932, 3340. 3,6-Bis(4-methoxyphenyl)-furo[3,2-b]furan-2,5-dione (**7**) [32]. Sodium (3.6 g, 156 mmol, 2 eq) was dissolved in cooled absolute ethanol (50 mL). Diethyl oxalate (10.8 mL, 80 mmol, 1 eq) and 4-methoxyphenylacetonitrile (22.6 mL, 156 mmol, 2 eq) were added after complete consumption of the sodium. The mixture was stirred at  $70^\circ\text{C}$  for 90 min, and cooled to room temperature. Water (8 mL) were added, followed by acidification with acetic acid down to pH 5. This led to the precipitation of 9.55 g of an orange product. This was dissolved in 20 mL of acetic acid and 10 mL of water before adding dropwise 8.5 mL of concentrated sulfuric acid. A red solid appeared, and the mixture was heated at reflux for 30 min after which it was cooled in an ice bath. The solid was collected by filtration, suspended in 15 mL of acetic anhydride and heated at reflux for 30 min. The bis-lactone **7** was collected at room temperature by filtration and washed with heptane. Yield: 10%.  $^1\text{H}$  NMR (400 MHz,  $\text{CDCl}_3$ ):  $\delta = 3.89$  (s, 6H), 7.01 (d, 4H,  $J = 8.6$  Hz), 8.01 (d, 2H,  $J = 8.6$  Hz);  $^{13}\text{C}$  NMR ( $\text{CDCl}_3$ ):  $\delta = 54.8, 96.4, 100.3, 115.3, 117.6, 130.0, 134.4, 159.5$ ; IR ( $\text{cm}^{-1}$ ): 595, 869, 1019, 1157, 1257, 1354, 1506, 1600, 1657, 1782, 1909.



2.1.7. (*E*)-*N*-(2-(1,4,7,10,13-Pentaoxa-16-azacyclooctadecan-16-yl)ethyl)-2-(3-hydroxy-4-(4-methoxyphenyl)-5-oxofuran-2(5*H*)-ylidene)-2-(4-methoxyphenyl)acetamide (**8**)

2-Aminomethyl-18-crown-6 (250 mg, 0.85 mmol, 1.1 eq) was added to a suspension of compound **7** (270 mg, 0.77 mmol) in 15 mL of DCM. The mixture was stirred for 1 h at room temperature and concentrated. The crude was purified by chromatography (DCM/MeOH 98/2) to give **8** as an orange solid. Yield: 93%.  $^1\text{H}$  NMR ( $\text{CDCl}_3$ ):  $\delta$  = 3.48–3.72 (m, 25H), 3.82 (s, 3H), 3.83 (s, 3H), 6.76 (s, 1H), 6.94 (d, 2H,  $J$  = 9.2 Hz), 6.97 (d, 2H,  $J$  = 8.8 Hz), 7.22 (d, 2H,  $J$  = 8.8 Hz), 8.12 (d, 2H,  $J$  = 8.8 Hz);  $^{13}\text{C}$  NMR:  $\delta$  = 42.4, 55.4, 55.4, 69.5, 70.7–71.0 (m), 72.2, 103.1, 113.9, 114.7, 117.1, 122.6, 124.1, 129.0, 131.6, 152.7, 159.1, 160.3, 160.9, 167.4, 168.9; HRMS (ESI): *Anal. Calc.* for  $\text{C}_{33}\text{H}_{42}\text{NO}_{12}$  ( $[\text{M}+\text{H}]^+$ ): 644.27015. Found: 644.27263%; IR: ( $\text{cm}^{-1}$ ): 463, 486, 522, 549, 582, 634, 650, 699, 752, 765, 828, 880, 912, 956, 1024, 1110, 1182, 1247, 1292, 1417, 1444, 1463, 1506, 1556, 1601, 1766, 1860, 2863, 2895, 2942, 3373, 3398.

2.2. Stock solutions

The ethanol-to-water ratio is given in volume. The solubilities of B1 and B2 are very poor in water. Therefore, both molecules were first dissolved in pure ethanol ( $5 \times 10^{-4}$  M) and then diluted in the final media to  $[1-100] \times 10^{-7}$  M and  $[5-100] \times 10^{-7}$  M, respectively. All other products were of the purest possible grade (Sigma, Merck, Acros, or Aldrich). Ethanol was Merck spectroscopy grade, and water was demineralized and doubly distilled.

2.3. Spectrophotometric measurements

Absorption measurements were performed at  $25 \pm 0.1$  °C on a Cary 4000 spectrophotometer equipped with Peltier thermostated cell-carriers. Fluorimetric measurements were performed at  $25 \pm 0.5$  °C on an Amino-Bowman series 2 luminescence spectrometer equipped with a thermostated cell carrier. The fluorescence intensity was corrected for the inner filter effect of the absorption of B1 and B2.

2.4. pH Measurements

The pHs were measured at  $25 \pm 0.5$  °C with a Jenco pH-meter. In M1 (ethanol/water 9/1) and EtOH, the pH values were corrected according to published procedures [33].

2.5. Protodissociation and affinity constants measurements

Protodissociations and affinity constants were determined spectrophotometrically by the use of the Global Analysis program SPECFIT32. SPECFIT32 is a multivariate data analysis program for data sets that are obtained from multiwavelength spectrophotometric measurements. The program utilizes a specially adapted version of the Levenberg–Marquardt method. This procedure returns optimized model parameters, their standard errors, and the predicted spectra of the unknown colored species [34]. For protodissociations, the spectra were measured at different pH values in M1. Neutralization and acidification were achieved with NaOH

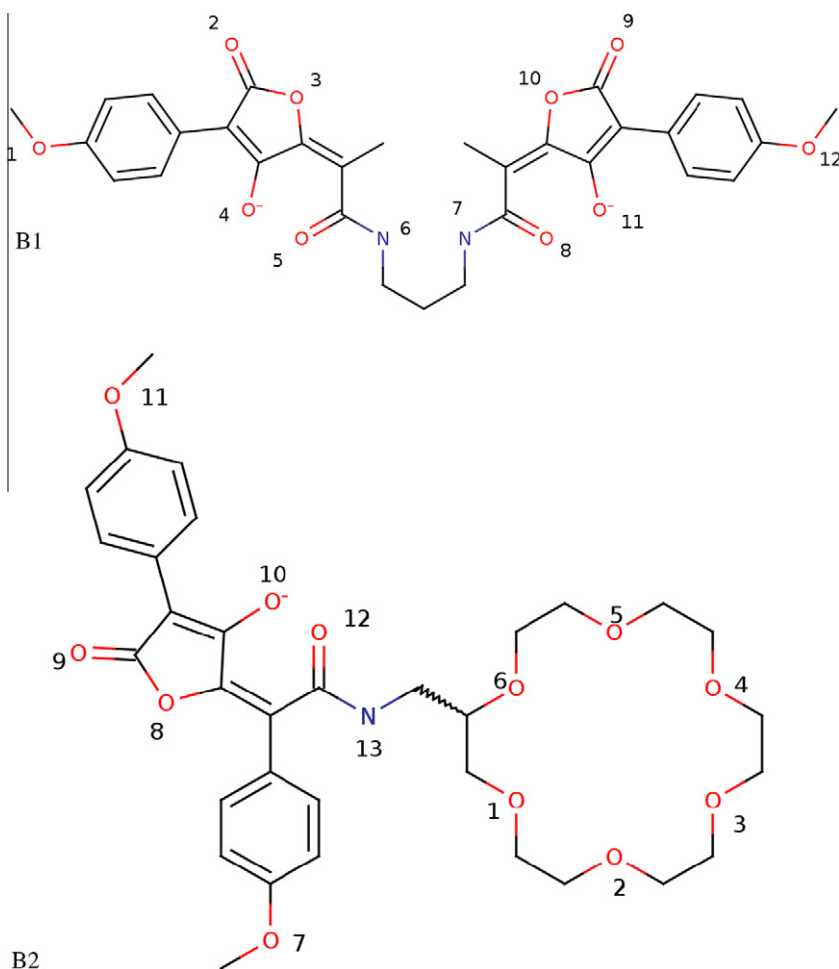


Fig. 2. Molecular structures of B1 and B2. The numbers represent the atom ID used in Tables 3–6.

( $\leq 1 \times 10^{-5}$  M) and HCl ( $\sim 1 \times 10^{-3}$  M). The affinity constants were checked when possible by a variant of the Benesi and Hildebrand method. Unless specified otherwise, they were measured in ethanol in the absence of alkali cations other than  $\text{Cs}^+$ ,  $\text{Na}^+$  or  $\text{K}^+$ . In M1, they were measured in media buffered with  $5 \times 10^{-4}$  M of boric acid at pH 9.3.

## 2.6. T-jump kinetics

Experiments were run on a modified Joule effect Messanlagen und Studien absorption and fluorescence emission T-jump spectrophotometer. The apparatus was equipped with a 200 W Xe/Hg light source, a Jarrel Ash monochromator, and a thermostated cell-holder maintained at  $20 \pm 1$  °C [18]. The temperature jump of 5–6 °C was achieved by discharging an 0.05  $\mu\text{F}$  condenser charged at 10 kV in solutions containing 0.1 M  $\text{NH}_4\text{Cl}$ .

## 2.7. Stopped-flow kinetics

Experiments were realized on a Hi-Tech Scientific SF61DX2 stopped-flow spectrophotometer equipped with a Xe/Hg light source and a thermostated bath at  $25 \pm 1$  °C. Solutions of B1 and B2 in water, M1 and EtOH ( $1 \times 10^{-7}$  M  $< c_0 < 5 \times 10^{-7}$  M) were mixed with solutions of  $\text{Cs}^+$  ( $0 < c_1 < 1 \times 10^{-3}$  M). All signals were accumulated at least 10 times. The excitation wavelength was set to 365 nm, which is one of the emission peaks of the light source. Detection was set to  $\lambda_{\text{em}} \geq 400$  nm.

## 2.8. Data analysis

The kinetic data were analyzed by linear and nonlinear least-squares regressions, and all uncertainties are twice the standard deviations. Brouillard established the conditions in which chemical relaxation approximations can apply with the use of high perturbations, such as concentration-jumps [35]. Therefore, all the experimental conditions were set so as to allow the use of the methods and techniques of chemical relaxation. This led to the fact that all the observed kinetic processes were pure exponentials and assumed as relaxation modes [18,19,35–38].

## 2.9. Molecular analysis simulation

SYBYL software was used for the graphical construction of B1 and B2 (Fig. 2) [39]. All calculations were performed with the AMBER v11 software package [40]. B2 contains an asymmetric carbon which led us to consider the two possible B2-R and B2-S isomers in our computational approach. The GAFF (general AMBER force field) [41] set of parameters was used with the atomic partial charges produced by AM1–BCC computations [42,43]. B1 and B2 were first optimized with 5000 steps of minimization in an ethanol implicit solvent with a dielectric constant of 24.4. A single cation ( $\text{Na}^+$ ,  $\text{K}^+$  or  $\text{Cs}^+$ ) ion, provided by the AMBER software [44], was afterwards randomly added. Molecular dynamics simulations at 300 K were carried out for 10 ns in ethanol implicit solvent, with each of the three cations for B1 and B2. Computational details are reported elsewhere [45]. To initiate the systems and facilitate the interaction between the cations and the ligands, weak restraints (10 kcal/mol max) were imposed for 2 ns. These were defined as a square-bottom potential well with parabolic sides up to an established distance, and linear afterwards. The distances between each ion and the oxygen atoms carrying the negative charges of B1 and the enolate of B2 were chosen as indicators for complex formation. This is based on the fact that electrostatic effects are long-range interactions. After 2 ns, all restraints were removed. Molecular imaging and structural analysis were then performed for the remaining 8 ns with the VMD software [46].

In all simulations, potential, kinetic and total energy were maintained constant. Furthermore, the restraint did not cause any steric hindrance. Cation interaction with the ligands occurred in less than 10 ps and the complexes did not dissociate after release of the restraint. This confirms the recognition potential of B1 and B2 for the three alkali cations.

## 3. Results

### 3.1. Synthesis

For the synthesis of B1 and B2, we expected to make use of the particular reactivity of bis-lactone type compounds. These compounds are obtained by dehydration of pulvinic acids (Scheme 1) [32]. In the presence of a nucleophile, and especially amines, one of the lactone functions will react by ring-opening, giving thus the two amides without any control of the regioselectivity (Scheme 2). In the case of bis-lactone 1, we recently reported that the addition of 2 equivalents of TBAF allows controlling the regioselectivity, giving compound 2 as the major product (Scheme 3) [31].

For compound B1, initially one equivalent of the bis-lactone 1 reacted with 0.5 equivalent of 1,3-diaminopropane in DCM. However, this led to the precipitation of intermediate 4, thus preventing the second attack of the free amine of 4. The addition of DMSO to solubilise the mixture allowed this second reaction, but led to the formation of three isomers (Scheme 4), which were inseparable by chromatography on silica gel. The reaction was then performed in the presence of TBAF in THF, which prevented the formation of isomers 5 and 6. B1 was isolated in 57% yield.

We then focused our attention on the synthesis of derivatives bearing a crown ether, choosing the commercially available amine 7 for an initial attempt. The reaction with bis-lactone 1 in the presence of TBAF in THF was not regioselective, giving the two isomers, which again were inseparable by chromatography on silica gel (Scheme 5).

In order to avoid regioselectivity problems, we selected bis-lactone 10, in which the two lactone moieties are identical. The reaction of amine 7 on 10 in DCM led to compound B2 in 93% yield (Scheme 6).

### 3.2. Thermodynamics

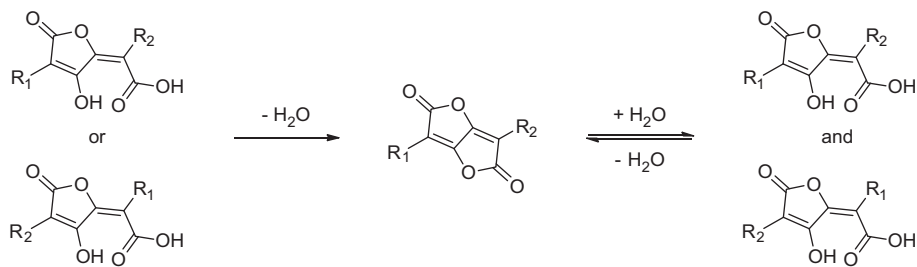
The results reported here are obtained in three different media: (1) water, (2) ethanol/water 9/1 in volume (M1) and (3) ethanol. We began by analyzing the protodissociations of the acid–base centers involved in B1 and B2, in the absence or presence of  $\text{Cs}^+$ ,  $\text{Na}^+$  or  $\text{K}^+$ , in water and M1. B1 and B2 have typical absorption and fluorescence emission spectra in water, M1 and EtOH. Therefore, spectrophotometric detection was used in most of our experiments.

#### 3.2.1. Protodissociation constants

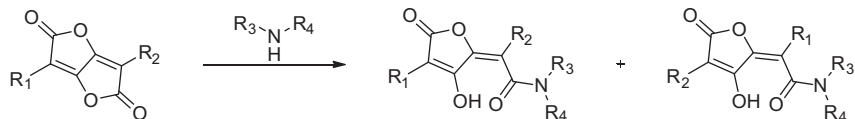
In M1, the absorption spectra of both B1 and B2 vary with pH (Fig. 3A and B). The analysis of the spectrophotometric data by the SPECFIT32 program allowed us to determine 2  $\text{pK}_a$  values (Eqs. (1) and (2)) for B1 and one  $\text{pK}_a$  value (Eq. (3)) for B2, which, as for NbA and its subunits, were ascribed to the enol functions (Table 1) [18]



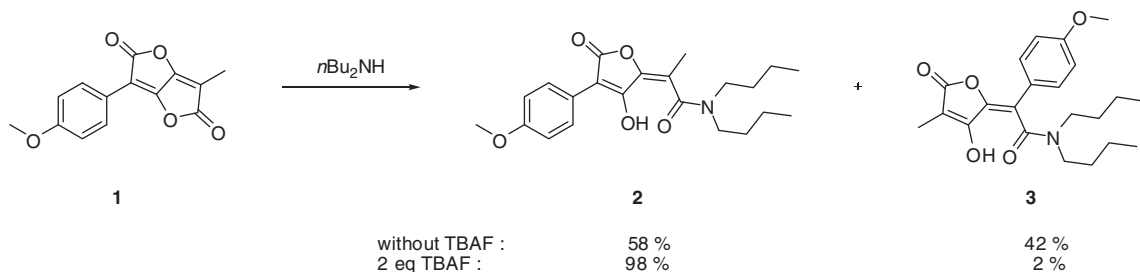
where  $\text{B1}^{2-}$  is the fully deprotonated B1 species,  $\text{B2}^-$  the fully deprotonated B2 species and  $\text{K}_{1a} = [\text{H}^+][\text{B1}^{2-}]/[\text{B1H}^-]$ ,  $\text{K}_{2a} = [\text{H}^+][\text{B1H}^-]/[\text{B1H}_2]$  and  $\text{K}_{3a} = [\text{H}^+][\text{B2}^-]/[\text{B2H}]$ .



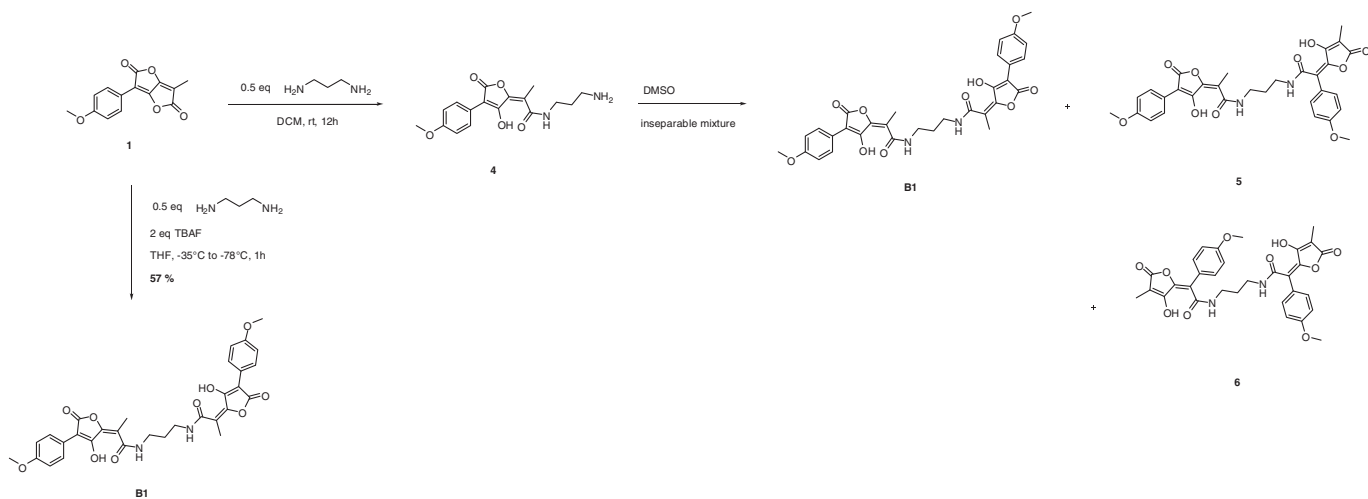
Scheme 1.



Scheme 2.



Scheme 3.

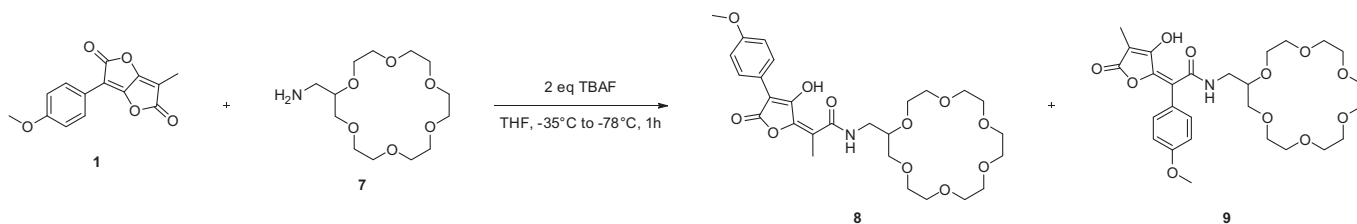


Scheme 4.

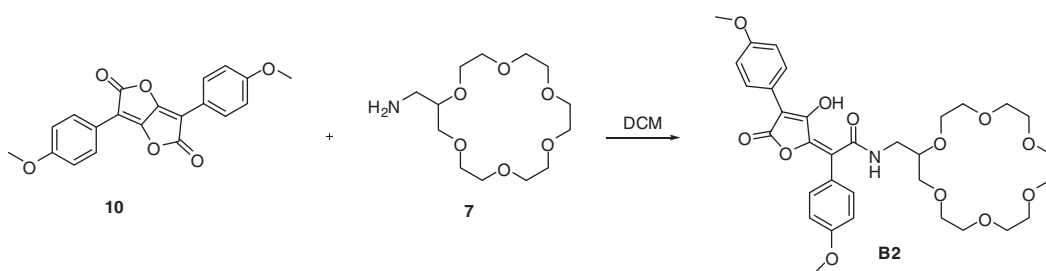
The same measurements were performed in an excess of  $\text{Cs}^+$ ,  $\text{Na}^+$  or  $\text{K}^+$  (not shown) at  $c_1 = 1 \times 10^{-2} \text{ M}$  with B1 and  $c_1 = 5 \times 10^{-5} \text{ M}$  with B2. In M1 and in the case of B1 and B2 in the presence of  $\text{Cs}^+$ ,  $\text{p}K_{1a}$ ,  $\text{p}K_{2a}$  and  $\text{p}K_{3a}$  are decreased by 0.5, 2.6 and 0.15 (Table 1), respectively. They kept the same values with  $\text{Na}^+$  and  $\text{K}^+$ . This implies that complex formation occurs between the alkali metal and the enolates [47].

### 3.2.2. Complex formation

In the 7–9.5 pH range and at fixed pH values, adding  $\text{Cs}^+$ ,  $\text{Na}^+$  or  $\text{K}^+$  to a B1 or B2 solutions in an aqueous medium does not lead to any change in the absorption or emission spectra. This does not imply that the  $\text{Cs}^+$  complexes are not formed with B1 or B2 in water. It means that if a complex is formed, it is not detected by the spectrophotometric techniques.



Scheme 5.



Scheme 6.

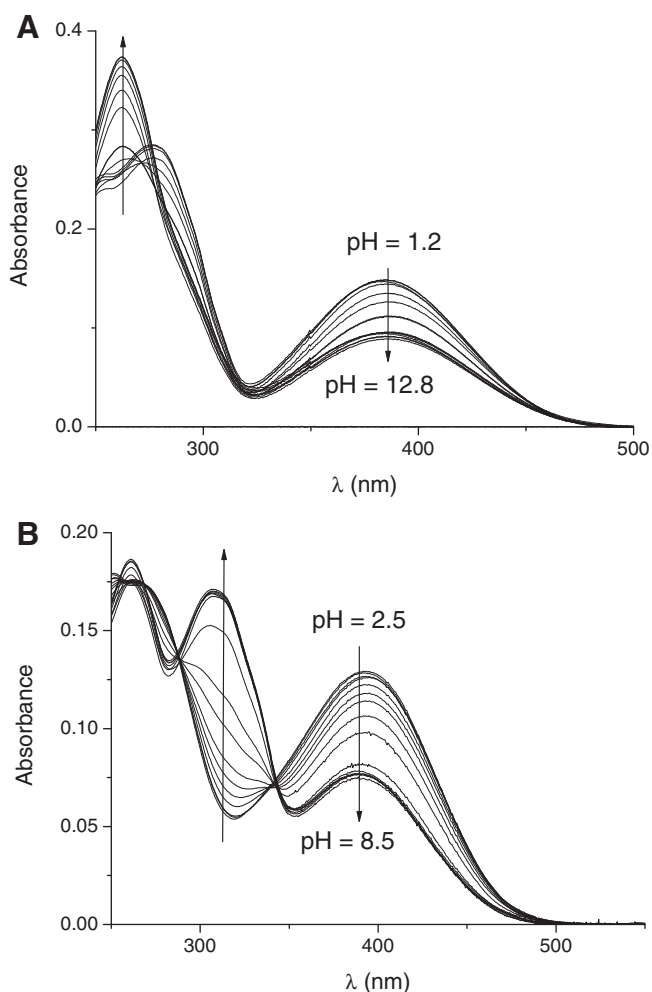


**Fig. 3.** Evolution of the absorption spectra with pH at  $25.0 \pm 0.5$  °C. (A) B1 ( $c_0 = 5 \times 10^{-6}$  M) in M1, (B) B2 ( $c_0 = 5 \times 10^{-6}$  M) in M1.

In M1 and EtOH, adding  $\text{Cs}^+$ ,  $\text{Na}^+$  or  $\text{K}^+$  to solutions of B1 and B2 leads to changes in the emission and differential absorption

Table 1

Protodissociation constants of B1 and B2 in the absence or presence of  $\text{Cs}^+$  ( $c_1 = 1 \times 10^{-2}$  M with B1 and  $5 \times 10^{-5}$  M with B2) in M1 at  $25.0 \pm 0.5$  °C.

		Without $\text{Cs}^+$	With $\text{Cs}^+$
B1	$\text{p}K_{1a}$	$5.6 \pm 0.1$	$5.1 \pm 0.3$
	$\text{p}K_{2a}$	$8.00 \pm 0.15$	$5.4 \pm 0.1$
B2	$\text{p}K_{3a}$	$4.60 \pm 0.05$	$4.40 \pm 0.05$

spectra of both ligands, with the metal-free ligands taken as references (Fig. 4A and B for  $\text{Cs}^+$ , not shown for  $\text{K}^+$  and  $\text{Na}^+$ ). If we assume that these changes are the results of complex formation between the alkali cations and B1 or B2, we can use the SPECFIT32 program to determine the stoichiometries and affinities involved [18,19,34]. In each case, the analysis implies a single complex formation (Eqs. (4) and (5)):



with  $\text{Ak}^+ = \text{Cs}^+$ ,  $\text{Na}^+$  or  $\text{K}^+$ ;  $K_{1B1} = [\text{B1Ak}^+]/[\text{B1}][\text{Ak}^+]$  and  $K_{1B2} = [-\text{B2Ak}^+]/[\text{B2}][\text{Ak}^+]$ . In ethanol and in M1,  $K_{1B1\text{EtOH}}$ ,  $K_{1B2\text{EtOH}}$ ,  $K_{1B1\text{M1}}$  and  $K_{1B2\text{M1}}$  are reported in Table 2 for the three  $\text{Ak}^+$ . These values were confirmed by a Benesi and Hildebrand analysis [18,19,48].

The addition of variable concentrations ( $c_1$ ) of alkali cations to B1 increases the fluorescence intensity up to a plateau at about  $c_1 \sim 1 \times 10^{-4}$ ,  $1 \times 10^{-4}$  and  $5 \times 10^{-4}$  M, for  $\text{Cs}^+$ ,  $\text{Na}^+$  and  $\text{K}^+$ , respectively. This is accompanied by a 10 nm blue shift (Fig. 5A for  $\text{Cs}^+$ , not shown for  $\text{K}^+$  and  $\text{Na}^+$ ). In M1, the fluorescence intensity increases up to a plateau for  $c_1 \sim 1.5 \times 10^{-4}$ ,  $1 \times 10^{-4}$  and  $5 \times 10^{-4}$  M, for  $\text{Cs}^+$ ,  $\text{Na}^+$  and  $\text{K}^+$ , respectively. This is accompanied by a 5 nm blue shift (Fig. 5B for  $\text{Cs}^+$ , not shown for  $\text{K}^+$  and  $\text{Na}^+$ ). The analysis of the emission spectra by the SPECFIT32 program allowed us to determine and confirm the  $K_{1B1\text{EtOH}}$  and  $K_{1B1\text{M1}}$  values (Table 2). The same experiments were repeated with B2. The addition of the alkali cations manifested by an increase in the fluorescence intensities without, however, the blue shifts observed for B1 (Fig. 6A and B for  $\text{Cs}^+$ , not shown for  $\text{K}^+$  and  $\text{Na}^+$ ). These results confirm those obtained by differential absorption detection (Table 2).

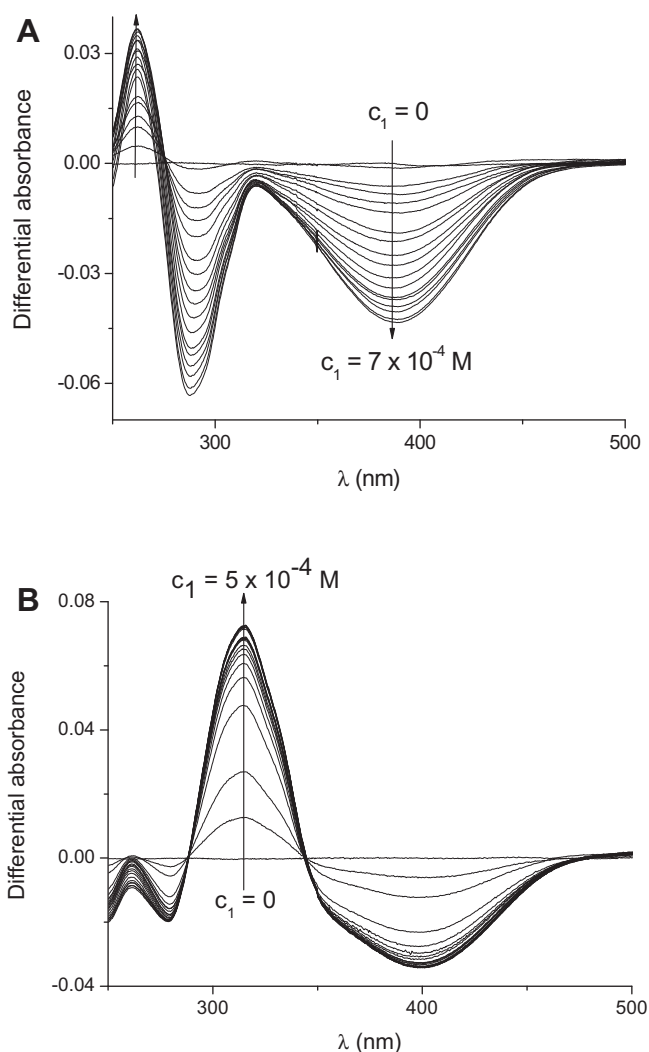


**Fig. 4.** Differential absorption spectra. (A) B1 in ethanol at different  $\text{Cs}^+$  concentrations with B1 taken as reference, with  $c_0 = 1 \times 10^{-5}$  M and  $0 < c_1 < 7 \times 10^{-4}$  M at  $25.0 \pm 0.5$  °C, (B) B2 in ethanol at different  $\text{Cs}^+$  concentrations with B2 taken as reference, with  $c_0 = 1 \times 10^{-5}$  M and  $0 < c_1 < 5 \times 10^{-4}$  M at  $25.0 \pm 0.5$  °C.

### 3.3. Kinetics

The spectrophotometric variations describing complex formation upon the addition of alkali cations to solutions of B1 and B2

in M1 and EtOH are too fast to allow kinetic detection by conventional techniques. Indeed, complex formation with alkalis is assumed to be an extremely fast process, which can be diffusion-controlled [15,17,49]. Our kinetic investigations were, therefore, first performed by T-jump and then by the stopped-flow mixing technique [18,19]. We did not succeed in obtaining exploitable results by T-jump (low signal-to-noise ratio and very small signal variations).

In EtOH, when solutions of B1 or B2 are mixed with solutions of  $\text{Cs}^+$ ,  $\text{Na}^+$  or  $\text{K}^+$ , a single kinetic process occurs as an exponential increase in the fluorescence intensity with time (excitation maximum,  $\lambda_{\text{ex}} = 365$  nm; emission  $\lambda_{\text{em}} > 400$  nm) (Fig. 7A and B for  $\text{Cs}^+$ , not shown for  $\text{K}^+$  and  $\text{Na}^+$ ). The experimental reciprocal relaxation times associated with these processes depend on  $[\text{Ak}^+]$ .

The reciprocal relaxation time equation associated with Eqs. (4), (5) is expressed as [18,19,36,37]:

$$\tau^{-1} = k_1([\text{Ak}^+] + [\text{B}]) + k_{-1} \quad (6)$$

with,  $\text{B} = \text{B1}$  or  $\text{B2}$ .

Since, under our experimental conditions,  $[\text{Ak}^+] \gg [\text{B}]$ , Eq. (6) simplifies to Eq. (7):

$$\tau^{-1} = k_1 c_1 + k_{-1} \quad (7)$$

with  $c_1$ , the analytical concentration of the alkali metal salt.

A very good linear least-squares regression of the data was obtained for each of the two ligands with  $\text{Cs}^+$ ,  $\text{Na}^+$  or  $\text{K}^+$  in EtOH (Fig. 8A and B for  $\text{Cs}^+$ , not shown for  $\text{K}^+$  and  $\text{Na}^+$ ). From the slopes and intercepts of the best lines,  $k_1$ ,  $k_{-1}$  and  $K = k_1/k_{-1}$  values were determined for B1 and B2 with each of the three alkali cations (Table 2). The  $K$  values are, within the limits of uncertainty, identical to those determined spectrophotometrically.

In M1, mixing solutions of B1 or B2 with solutions of  $\text{Cs}^+$ ,  $\text{Na}^+$  or  $\text{K}^+$  leads to very fast processes ( $< 1$  ms) resulting in an increase in the fluorescence emission. Attempts to use the T-jump technique to investigate these processes were fruitless, because the signal-to-noise ratios were too low to allow any interpretation. To obtain further information about the structures that may be involved in the alkali complexes, modeling of the B1- and/or B2- $\text{Cs}^+$  complexes was performed by molecular dynamics simulations.

### 3.4. Modeling

Two main conformations of the B1- $\text{Ak}^+$  complexes are extracted from the molecular dynamics trajectory. They correspond to a “cisoid/transoid” of the aromatic moieties (Fig. 9). The “cisoid”s

**Table 2**  
Kinetic and thermodynamic data related to complex formation between  $\text{Cs}^+$ ,  $\text{Na}^+$ ,  $\text{K}^+$  and B1 or B2 in EtOH and in M1 at pH 9.3.

Molecule	Metal	$\log K_{\text{B}_{\text{EtOH}}}$ <sup>a</sup>	$k_1$ ( $\text{M}^{-1} \text{s}^{-1}$ )	$k_{-1}$ ( $\text{s}^{-1}$ )	$\log K_{\text{B}_{\text{EtOH}}}$ <sup>b</sup>	$\log K_{\text{B}_{\text{M1}}}$ <sup>a</sup>
B1	$\text{Cs}^+$	$4.8 \pm 0.1^c$	$(1.2 \pm 0.1) \times 10^5$	$2 \pm 1$	$4.7 \pm 0.3$	$4.7 \pm 0.1^c$
		$5.0 \pm 0.3^d$				$4.9 \pm 0.2^d$
B2	$\text{Cs}^+$	$6.4 \pm 0.1^c$	$(2.1 \pm 0.1) \times 10^7$	$11 \pm 4$	$6.3 \pm 0.2$	$6.1 \pm 0.1^c$
		$6.3 \pm 0.1^d$				$6.0 \pm 0.2^d$
B1	$\text{Na}^+$	$5.0 \pm 0.1^c$	$(9.3 \pm 0.3) \times 10^5$	$17 \pm 2$	$4.7 \pm 0.2$	$4.9 \pm 0.1^c$
		$5.1 \pm 0.2^d$				$5.0 \pm 0.2^d$
B2	$\text{Na}^+$	$6.0 \pm 0.1^c$	$(1.4 \pm 0.1) \times 10^7$	$18 \pm 4$	$5.9 \pm 0.2$	$5.8 \pm 0.1^c$
		$5.8 \pm 0.2^d$				$5.7 \pm 0.2^d$
B1	$\text{K}^+$	$4.3 \pm 0.1^c$	$(4.7 \pm 0.4) \times 10^5$	$38 \pm 1$	$4.1 \pm 0.2$	$4.2 \pm 0.1^c$
		$4.3 \pm 0.1^d$				$4.1 \pm 0.2^d$
B2	$\text{K}^+$	$5.5 \pm 0.2^c$	$(9.1 \pm 0.2) \times 10^6$	$26 \pm 6$	$5.5 \pm 0.2$	$5.3 \pm 0.1^c$
		$5.6 \pm 0.3^d$				$5.1 \pm 0.2^d$

<sup>a</sup> Is related to the spectrophotometric determination of the  $K$  values.

<sup>b</sup> Is related to their kinetic determination.

<sup>c</sup> Is related to determination of the  $K$  values using differential absorption.

<sup>d</sup> Is related to their determination using fluorescence emission.

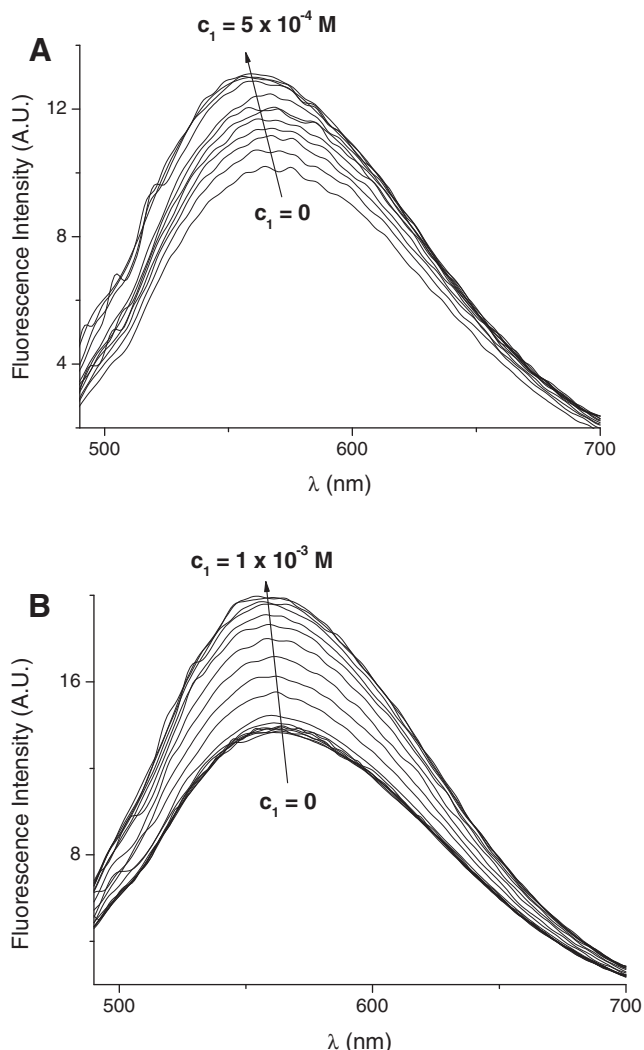


**Fig. 5.** Emission spectra of solutions of B1 at different  $\text{Cs}^+$  concentrations for  $\lambda_{\text{ex}} = 391 \text{ nm}$ ,  $c_0 = 1 \times 10^{-6} \text{ M}$  at  $25 \pm 0.5 \text{ }^\circ\text{C}$ . (A) EtOH with  $0 < c_1 < 5 \times 10^{-4} \text{ M}$ , (B) M1 with  $0 < c_1 < 1 \times 10^{-3}$ .

conformers are present for about 80% of the complex lifetime, whereas the “transoid”s are present for the remaining 20%. The “transoid”s are less stable than the “cisoid”s by about 4 kcal/mol (Table 3). These differences in energy are the consequence of van der Waals and electrostatic effects, which stabilize the “cisoid”s. The values of average energies of the systems are practically identical for the three cations, which implies that B1 binds all three (Table 3). In all three cases, the electrostatic term remains by far the main component of the potential energy, because of the two negative charges of the ligand. Comparison of the energies of the three  $\text{Ak}^+$  complexes is slightly in favor of  $\text{Na}^+$  (about 2 kcal/mol, Table 4). This is probably due to the van der Waals interactions which favor smaller ionic radii. Moreover, the average distances between the  $\text{Ak}^+$ /heteroatoms and the ligands (Table 4) are longer in the “transoid” conformation (6.41 Å for  $\text{Cs}^+$ ) than in the “cisoid” (6.29 Å for  $\text{Cs}^+$ ). This highlights a more favorable electrostatic effect in the “cisoid” conformer. Furthermore, the lifetime of the “transoid” is slightly longer with  $\text{Na}^+$ . This is probably due to its smaller ionic radius, which leads to less steric hindrance than with  $\text{K}^+$  and  $\text{Cs}^+$ .

The enantiomers  $\text{B2R-Ak}^+$  and  $\text{B2S-Ak}^+$  complexes each adopt a conformation in which the cation is surrounded by the oxygens of the crown ether and capped with the aromatic part of the molecule (Fig. 10). This capping maximizes the electrostatic interaction

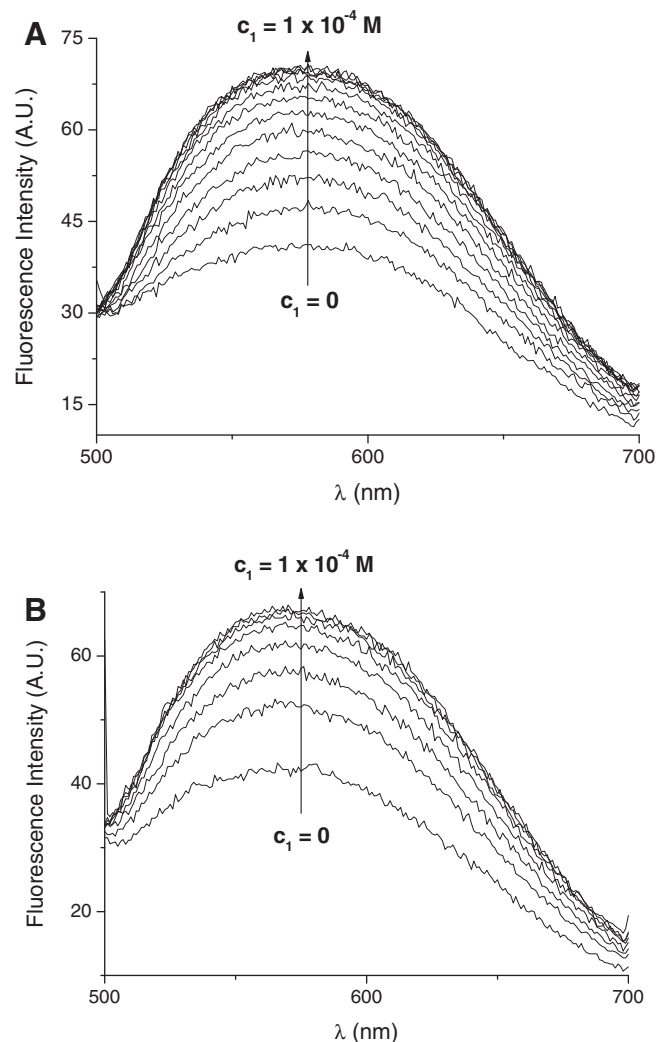


**Fig. 6.** Emission spectra of solutions of B2 at different  $\text{Cs}^+$  concentrations for  $\lambda_{\text{ex}} = 391 \text{ nm}$ ,  $c_0 = 1 \times 10^{-6} \text{ M}$  at  $25 \pm 0.5 \text{ }^\circ\text{C}$ . (A) EtOH with  $0 < c_1 < 1 \times 10^{-4} \text{ M}$ , (B) M1 with  $0 < c_1 < 1 \times 10^{-4}$ .

between the enolate and the positive charge of the cation. Similar 3D structures for the  $\text{B2R-}$  and  $\text{B2S-Ak}^+$  are not surprising (Table 5). In fact, the crown ether linked to the asymmetric carbon is very flexible. It adopts, though variation of dihedral angle, two structures in which the oxygen atoms are equally exposed to provide the highest electrostatic stabilization. This is confirmed by the inter-atomic distances (Table 6) and by the energies (Table 5). These show that  $\text{B2R}$  is less stable by about 3 kcal/mol than  $\text{B2S}$ . This difference can be explained by the dihedral energy variation. It is, moreover, weak which allows the interaction of both enantiomers with the cations. Furthermore, B2 interacts strongly with the three cations. The differences in energy follow the ionic radius. Although the electrostatic effect is the major partner in these complexes, the van der Waals interactions are responsible for these variations in energy, as they slightly favor the  $\text{Na}^+$  complex at the expense of those with  $\text{K}^+$  and  $\text{Cs}^+$ .

## 4. Discussion

### 4.1. Complex formation

In Table 2, we summarize the kinetic and thermodynamic data determined here. The kinetic runs were performed by the

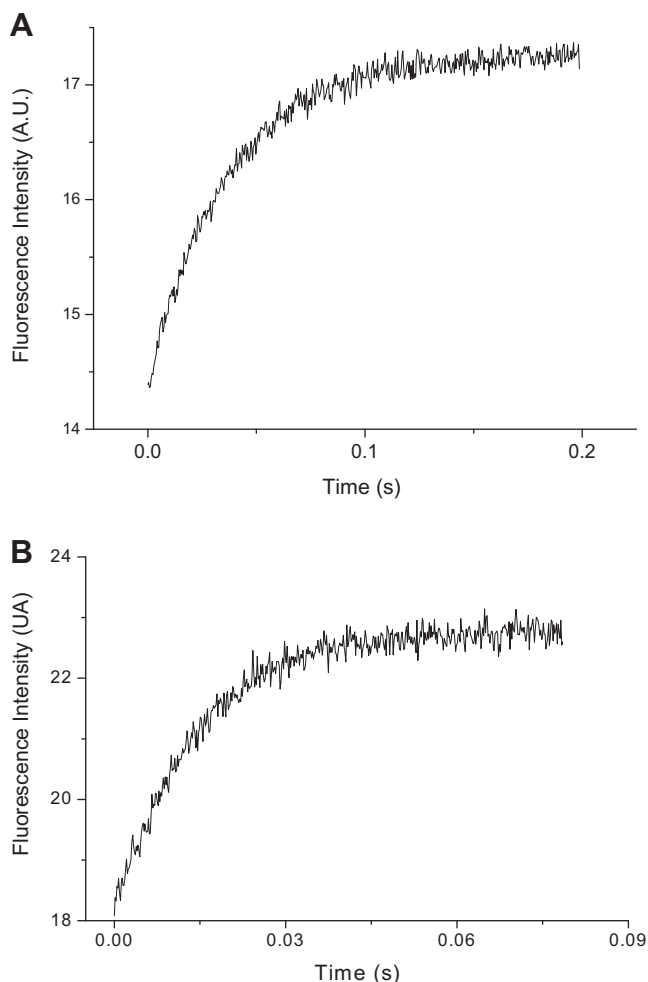


**Fig. 7.** Variation of the fluorescence emission with time for  $\lambda \geq 400$  nm at  $\lambda_{\text{ex}} = 365$  nm after stopped-flow mixing in ethanol at  $25.0 \pm 0.5$  °C of a solution of: (A) B1 ( $c_0 = 5 \times 10^{-7}$  M) with a solution of  $\text{Cs}^+$  ( $c_1 = 4 \times 10^{-4}$  M) and (B) B2 ( $c_0 = 5 \times 10^{-7}$  M) with a solution of  $\text{Cs}^+$  ( $c_1 = 4 \times 10^{-6}$  M).

stopped-flow mixing technique, which allows to investigate kinetic processes occurring in the  $10^{-3}$ –1 s range. Complex formation with alkali metals usually occurs by inclusion of the cation in the cavity of a crown ether or a calixarene [22,25,50,51]. Very few examples concerning complex formation between more classical ligands not bearing an inclusion cavity, such as NbA, are known [16,18,52]. The case of NbA is, therefore, rather unusual, as ligands such as enols and carboxylates form stable complexes with  $\text{Cs}^+$  and less stable ones with  $\text{Na}^+$  and  $\text{K}^+$  [18,52]. Furthermore, complex formation with alkali is believed to occur in the nano- to microsecond range and was studied mainly by the use of fast kinetic techniques, such as pulse and resonance ultrasonic relaxation or T-jump [15–19,53]. However, in the case of some capped calixarenes and NbA, complex formation with  $\text{Cs}^+$  is slowed down [18–20]. The rate constants in Table 2 are comparable to some of those reported for complex formation between cesium and NbA as well as a series of 2 crown[6]calyx[4]arenes in water, water–ethanol and ethanol. These rate constants increased from  $10^5 \text{ M}^{-1} \text{ s}^{-1}$  to  $6 \times 10^9 \text{ M}^{-1} \text{ s}^{-1}$  with the ethanol/water ratio up to M1. This was attributed to several factors, such as the rigidity of the calixarene or slow conformational changes, which allow the pulvinic acids of NbA to mimic an inclusion cavity [18,19]. This, however, is not the case here because in B1 and B2, conformational changes, would be extremely fast processes. Indeed, these two molecules do not present any structural

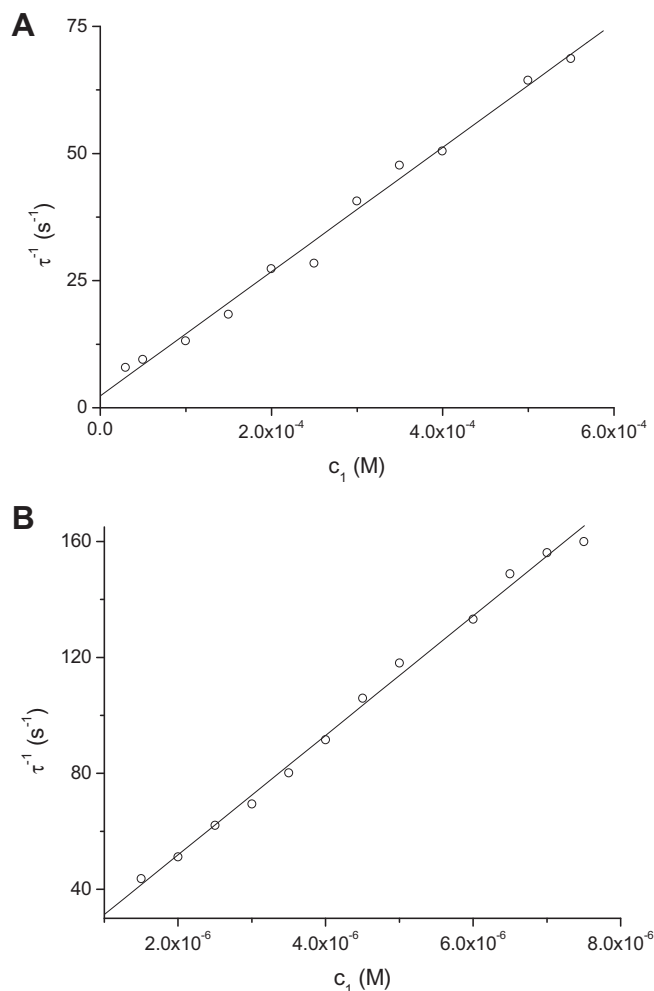


**Fig. 8.** Plot of  $\tau^{-1}$  against  $c_1$  after stopped-flow mixing in ethanol at  $25.0 \pm 0.5$  °C of a solution of: (A) B1 ( $c_0 = 5 \times 10^{-7}$  M) with solutions of  $\text{Cs}^+$ . Intercept,  $2 \pm 1 \text{ s}^{-1}$ ; slope,  $(1.22 \pm 0.07) \times 10^5 \text{ M}^{-1} \text{ s}^{-1}$ ;  $r = 0.99529$ , (B) B2 ( $c_0 = 5 \times 10^{-7}$  M) with solutions of  $\text{Cs}^+$ . Intercept,  $11 \pm 4 \text{ s}^{-1}$ ; slope,  $(2.1 \pm 0.1) \times 10^7 \text{ M}^{-1} \text{ s}^{-1}$ ;  $r = 0.99178$ .

rigidities or steric hindrances as in NbA or capped calixarenes. Nevertheless, although, highly improbable, if conformational changes were to rate-limit complex formation, the experimental relaxation times would be first order processes. In this case, they should be independent of the concentrations of the species present in the medium [18,19,35–38]. This would be in a total contradiction with our data as it is clearly shown that the experimental reciprocal relaxation times depend on alkali metal concentrations and are related to complex formation (Figs. 7 and 8; Eqs. (4), (5), and (7)). This is confirmed by the fact that the thermodynamic constants determined kinetically are within the limits of uncertainty identical to those reported by spectrophotometric titration (Table 2). In M1, these complex formations become much too fast (probably diffusion-controlled) to be measured.

The structure of B1 resembles that of NbA, with the two tetronic moieties assembled through a propyldiamide but without the naphthoquinone and the carboxylic ligand involved in the second  $\text{Cs}^+$  uptake by NbA [18]. However, in B1 the tetronic acids have certain flexibility, which is not the case in the separate moieties.  $\text{Na}^+$ ,  $\text{K}^+$  and  $\text{Cs}^+$  can be considered as rather hard metals, which implies the important role played by the oxygen ligands in complex formation with NbA [19,54]. The flexibility of the two tetronic moieties and the fact that the apparent  $\text{pK}_a$ s of the enols are affected by complex formation with  $\text{Cs}^+$  (Table 1) lead to the assumption of a

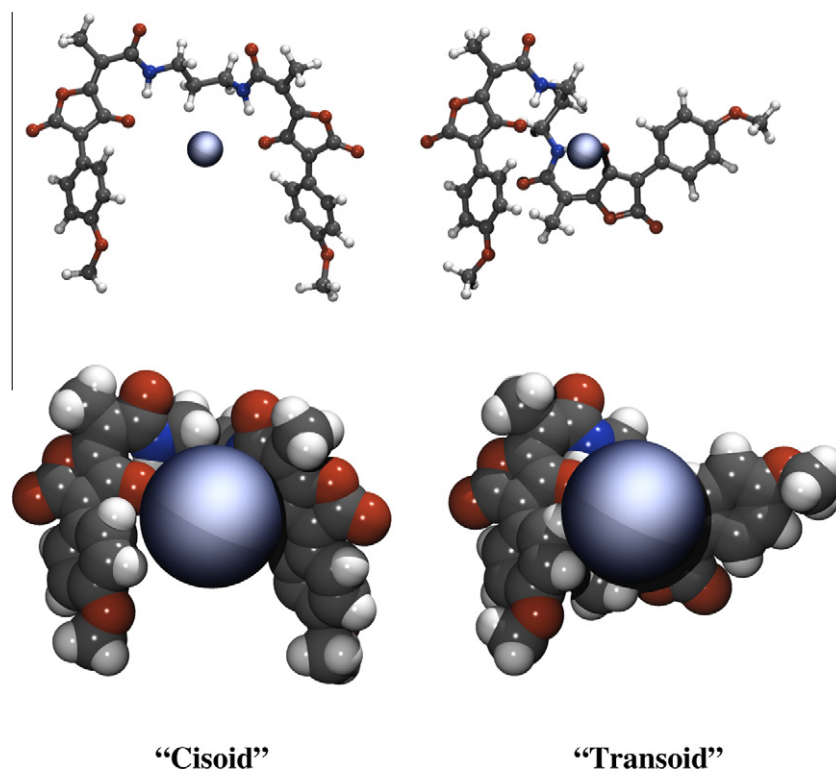


Fig. 9. Structures of the “cisoid” and “transoid” conformations of the  $\text{Cs}^+$  complex of B1, with ball and stick (top) and VDW (bottom) representations.

Table 3

Molecular energies of B1-Ak<sup>+</sup>, in kcal/mol, for the “cisoid” and “transoid” conformations. The time percentage stands for the presence ratio during the molecular dynamics trajectories.

Ion	Cisoid			Transoid			Average		
	Na <sup>+</sup>	K <sup>+</sup>	Cs <sup>+</sup>	Na <sup>+</sup>	K <sup>+</sup>	Cs <sup>+</sup>	Na <sup>+</sup>	K <sup>+</sup>	Cs <sup>+</sup>
% time	78	80	85	22	20	15	–	–	–
Epot	–280.14	–278.17	–276.81	–276.82	–274.47	–273.67	–279.41	–277.43	–276.34
Ebond	16.95	17.04	17.06	16.71	16.07	17.19	16.90	16.85	17.08
Eangle	51.74	52.98	53.08	52.02	53.20	52.74	51.80	53.03	53.03
Edihed	31.67	31.13	31.05	32.01	32.88	32.02	31.74	31.48	31.20
Evdw	–3.35	–2.11	–0.82	–2.53	–1.11	–0.06	–3.17	–1.91	–0.71
Eelec	–377.22	–377.34	–377.35	–375.12	–375.62	–375.72	–376.75	–377.00	–377.11
Erestr	0.07	0.13	0.18	0.08	0.11	0.16	0.07	0.13	0.18

Table 4

Distances, in Å, between Ak<sup>+</sup> and heteroatoms in the B1 complex. The inter atomic distance ID is displayed in Fig. 1.

ID/ conformation	Na <sup>+</sup>		K <sup>+</sup>		Cs <sup>+</sup>	
	Cisoid	Transoid	Cisoid	Transoid	Cisoid	Transoid
1	9.14	8.41	9.13	8.42	9.16	8.44
2	7.43	7.19	7.47	7.18	7.41	7.2
3	6.02	6.09	6.01	5.98	6.05	6.02
4	4.01	3.79	3.99	3.91	4.04	3.85
5	5.52	6.61	5.59	6.49	5.51	6.53
6	4.41	5.85	4.39	5.74	4.41	5.7
7	5.22	5.34	5.19	5.39	5.19	5.41
8	6.71	7.19	6.81	7.21	6.74	7.22
9	8.53	8.27	8.51	8.31	8.54	8.28
10	7.64	7.41	7.67	7.49	7.62	7.39
11	4.03	4.1	4.11	4.01	4.06	4.06
12	6.69	6.81	6.64	6.68	6.71	6.79
Average	6.28	6.42	6.29	6.40	6.29	6.41

complex with the enols in the deprotonated states. Therefore, the affinities for the three alkali cations were measured at pH 9.3, where all the enols are deprotonated.

#### 4.2. Modeling and proposed structures

Although, molecular dynamics simulations provide a supplementary temporal dimension to explore molecular flexibility, they are always performed in the ns scale with initial (2 ns in our case) weak restraints imposed on the system in explicit solvents. This is meant to impose an initial approach between the metal and the ligand. When the restraints are removed, the metal is released and becomes free to interact or not with the ligand for the remaining time (8 ns in our case). This time is short when compared to that of complex formation which, as already mentioned, occurs in the  $\mu\text{s}$  to the ms range (Table 2, Figs. 7 and 8). However, the molecular dynamics simulations available in the ms scales with no initial restraints validated approaches, such as ours [55–57]. These simulations were all performed with ANTON, a massively parallel supercomputer designed for molecular dynamics simulations of proteins and other biological macromolecules [58]. Therefore, although our models do not pretend to propose structures for the final complexes, they nevertheless constitute a realistic approach of these structures. In B1, the affinities are surprisingly high for alkali metals complexes, which do not involve an inclusion process

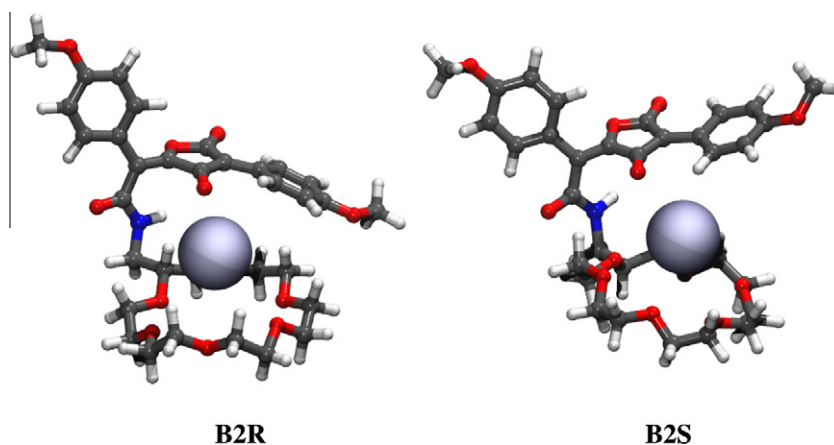


Fig. 10. Structures of B2–Cs<sup>+</sup> complexes.

Table 5

Molecular energies of B1, in kcal/mol, for the “cisoid” and “transoid” conformations. The time percentage stands for the presence ratio during the molecular dynamics trajectories.

	B2-R			B2-S		
	Na <sup>+</sup>	K <sup>+</sup>	Cs <sup>+</sup>	Na <sup>+</sup>	K <sup>+</sup>	Cs <sup>+</sup>
10	–71.70	–68.66	–65.52	–75.65	–71.22	–68.15
Ebond	18.86	19.19	18.72	18.69	19.17	19.10
Eangle	52.13	53.61	51.86	51.64	53.45	52.69
Edihed	38.63	38.35	39.65	35.61	36.03	36.57
Evdw	–9.19	–6.35	–5.52	–8.90	–6.10	–5.03
Eelec	–172.22	–173.67	–170.78	–172.80	–173.82	–171.73
Erestr	0.08	0.21	0.55	0.11	0.05	0.25

Table 6

Distances, in Å, between Ak<sup>+</sup> and the heteroatoms in the B2 complex. The ID is displayed in Fig. 1.

ID/ion	B2-R			B2-S		
	Na <sup>+</sup>	K <sup>+</sup>	Cs <sup>+</sup>	Na <sup>+</sup>	K <sup>+</sup>	Cs <sup>+</sup>
1	3.04	2.93	4.03	2.86	3.03	3.57
2	2.83	3.11	3.61	3.02	3.14	3.96
3	2.86	3.12	3.68	3.06	2.96	3.80
4	2.91	3.09	3.68	3.12	3.32	4.11
5	2.41	2.97	3.73	2.74	3.28	4.09
6	2.59	3.06	4.09	2.56	3.22	4.08
7	10.58	11.45	11.70	10.11	10.24	10.48
8	6.28	7.16	7.61	6.10	7.12	7.32
9	7.17	7.75	8.27	7.31	7.79	8.31
10	3.86	3.78	4.08	3.87	3.80	3.86
11	8.09	7.68	7.23	8.23	7.94	7.62
12	6.10	6.27	6.76	5.83	6.01	6.16
13	5.63	6.81	6.27	5.34	5.54	5.58
Average	4.95	5.32	5.75	4.93	5.18	5.61

in a crown ether or a calixarene [16]. The models proposed in Fig. 9 show that in B1 (Fig. 1 and Table 4), the alkali metals are very close to oxygens 4 and 11 (enolates), close to oxygen 5 (one of the two carbonyls) and to nitrogens 6 and 7 (diamide). This probably implies that a complex is formed between the alkali metals and the two enolates, one of the carbonyls and the diamide, which can in this case explain the values of the rather high affinity constants (Table 2). In NbA, complex formation occurs with two Cs<sup>+</sup>, the first with the enolates and the second with the carboxylates at higher pH values [18]. Complex formation between Cs<sup>+</sup> and NbA involves the Z and E conformers with a broad diversity of binding modes [59]. In the case of B1, the naphthoquinone and the carboxylic

acids are missing, which implies a monocomplex formation between the alkali metal and the enolates and leads to the cisoid and transoid conformations, with a preference for the cisoid's because it mimics an inclusion cavity (Fig. 9).

#### 4.3. Role of the crown ether

B2 contains a tetronic acid moiety and an 18-crown-6 ether. Crown ethers are good ligands for alkali cations, with which they form stable inclusion complexes [15,16,49,53,60]. Our aim was to synthesize a specific Cs<sup>+</sup> ligand by associating host–guest inclusion with a more classical coordination. The result was a ligand with higher affinities for Cs<sup>+</sup> than crown ethers, which can be compared to that of more specific Cs<sup>+</sup> ligands, such as calixarenes [22,23,51,61–63]. B2 is, however, also a good ligand for K<sup>+</sup> and Na<sup>+</sup> in M1 and a bit more selective for Cs<sup>+</sup> in EtOH (about one order of magnitude) (Table 2). Although molecular dynamics calculations are based on electrostatic and van der Waals interactions, they clearly imply that the B2–Cs<sup>+</sup> complex is present in ethanol in two conformations (Fig. 10, Table 6). The inter-atomic distances (Table 6) between Cs<sup>+</sup> and the oxygens of the crown ether are very close to those reported in the literature for the crystal structures of similar molecules [64]. The addition of the tetronic acid moiety stabilizes the inclusion complex by forming in both conformers a structure in which Cs<sup>+</sup> is included in the crown ether and interacts at the same time with amide 13 and oxygens 2–4. The interatomic distances involved in the more stable conformer B2S–Ak<sup>+</sup> (Fig. 10) and its lifetime (80% of that of the complex) indicate that the enol of the tetronic moiety acts as a supplementary arm which tends to cap Cs<sup>+</sup> and maintains it included in the crown ether. This also occurs with B2R–Ak<sup>+</sup> with, however, a lower lifetime. This explains the higher affinity of B2 for Cs<sup>+</sup> as compared to that of simple 18-crown-6 ethers [17].

#### 4.4. Mimicking NbA?

NbA forms strong complexes with Cs<sup>+</sup> in alcohol and water–alcohol mixtures. These complexes involve the two enolates and the two carboxylates. Complex formation occurs with one Cs<sup>+</sup> when only the enols are in the ionized state and with two Cs<sup>+</sup> when both the enol and the carboxylic acid moieties are deprotonated. This affinity of NbA for Cs<sup>+</sup> is probably the result of the particular structure in which the two pulvinic acid arms adopt a conformation that forms two complexation sites consisting of the two enolates and/or the two carboxylates [18]. In B1, a flexibility of the pulvinic ligand was sought to mimic an inclusion pseudocavity

or to adopt the structure of a pair of jaws that would surround the alkali metal. This is also implied by molecular dynamics, where the B1–Cs<sup>+</sup> complex in ethanol appears as two conformers, “transoid” and “cisoid” (Table 4 and Fig. 9). The latter is more stable than the “transoid” (Table 3). The “cisoid” conformation mimics, as expected here and assumed for NbA, an inclusion cavity in which the alkali cation is complexed by the enolate and carboxylate ligands. However, this flexibility does not increase the affinity of B1 for Cs<sup>+</sup> as compared to NbA [18]. With B1 a monocomplex is formed with K<sup>+</sup>, Na<sup>+</sup> and Cs<sup>+</sup> and the two enols. Furthermore, the affinities involved for the three alkali metals are within the same order of magnitude, whereas NbA shows specificity for Cs<sup>+</sup> (Table 2) [18]. The lack of the carboxylates does not explain the lack of selectivity for Cs<sup>+</sup>. With NbA this selectivity is the result of the positioning of the pulvinic acids imposed by the naphthol and the presence of the two carboxylic acid moieties which enables the molecules to complex two Cs<sup>+</sup> (Table 2) [18].

The results obtained with B2 are interesting, as the affinities for Cs<sup>+</sup> are higher than those with NbA and those with the crown ether alone ( $K_{1\text{crownEtOH}} \sim 1 \times 10^5$ ).

## 5. Conclusion

The decontamination of <sup>137</sup>Cs<sup>+</sup> following nuclear incidents, such as Chernobyl and Fukushima, remains a major public health problem. To the best of our knowledge, the elimination of this radioisotope is not yet possible. In nature, NbA is among the few molecules which form stable complexes with Cs<sup>+</sup>. To mimic its structure in order to achieve such a purpose is of interest. This is shown here by the capabilities of B1 and B2 to form stable complexes with alkali metals. Even if with B2 a slight specificity for Cs<sup>+</sup> is obtained, it remains that both B1 and B2 are not as specific for Cs<sup>+</sup> as envisaged. However, they constitute a framework which, with the involvement of the naphthol present in NbA, can lead to more specific Cs<sup>+</sup> chelators.

## Acknowledgment

This work was supported by DGA (Délégation Générale pour l'Armement) Grant PEA PROPERGAL N°. 06.70.110. The authors are grateful to Dr. John S. LOMAS for helpful discussions.

## References

- [1] Toxicology profile for cesium in: Agency Toxic Substances and Disease Registry (Ed.), US Department of Health and Human Services, 2004.
- [2] P. Melnikov, L.Z. Zononi, *Biol. Trace Elem. Res.* 135 (2010) 1.
- [3] Y. Jiang, Y. Feng, Y. Wang, J. Lu, M. Hu, S. Li, *Chem. Biol. Interact.* 171 (2008) 325.
- [4] F. Brown, G.R. Hall, A.J. Walter, *J. Inorg. Nucl. Chem.* 1 (1955) 241.
- [5] Chernobyl's Legacy in: Health, Environmental and Socio-Economic Impacts and Recommendations to the Governments of Belarus, the Russian Federation and Ukraine (Ed.), International Atomic Energy Agency D.K.I. Division of Public Information Austria, 2006.
- [6] A. Bolsunovsky, D. Dementyev, *J. Environ. Radioact.* 102 (2011) 1062.
- [7] D. Butler, *Nature* 472 (2011) 13.
- [8] D. Butler, *Nature* 471 (2011) 555.
- [9] D. Butler, *Nature* 472 (2011) 400.
- [10] D.C. Auman, G. Clooth, B. Steffan, W. Steglich, *Angew. Chem., Int. Ed. Engl.* 28 (1989) 453.
- [11] B. Steffan, W. Steglich, *Angew. Chem., Int. Ed. Engl.* 23 (1984) 445.
- [12] W. Steglich, W. Furtner, A. Prox, *Z. Naturforsch.* 23b (1968) 1044.
- [13] W. Steglich, W. Furtner, A. Prox, *Z. Naturforsch.* 25b (1970) 557.
- [14] M. Winner, A. Giménez, H. Schmidt, B. Sontag, B. Steffan, W. Steglich, *Angew. Chem., Int. Ed. Engl.* 43 (2004) 1883.
- [15] P.B. Chock, F. Eggers, M. Eigen, R. Winkler, *Biophys. Chem.* 6 (1977) 239.
- [16] M. Eigen, G. Maass, *Z. Phys. Chem.* 49 (1966) 163.
- [17] G.W. Liesegang, M.M. Farrow, N. Purdie, E.M. Eyring, *J. Am. Chem. Soc.* 98 (1976) 6905.
- [18] A. Korovitch, J.B. Mulon, V. Souchon, I. Leray, B. Valeur, A. Mallinger, B. Nadal, T. Le Gall, C. Lion, N.T. Ha-Duong, J.M. El Hage Chahine, *J. Phys. Chem. B* 114 (2010) 12655.
- [19] A. Korovitch, J.B. Mulon, V. Souchon, C. Lion, B. Valeur, I. Leray, N.T. Ha-Duong, J.M. El Hage Chahine, *J. Phys. Chem. B* 113 (2009) 14247.
- [20] Y. Suzuki, H. Otsuka, A. Ikeda, S. Shinkai, *Tetrahedron Lett.* 38 (1997) 421.
- [21] U.C. Meier, C. Detellier, *J. Phys. Chem. A* 103 (1999) 9204.
- [22] Z. Asfari, C. Bressot, J. Vicens, C. Hill, J.F. Dozol, H. Rouquette, S. Eymard, V. Lamare, B. Tournois, *Anal. Chem.* 67 (1995) 3133.
- [23] Z. Asfari, C. Naumann, J. Vicens, M. Nierlich, P. Thuery, C. Bressot, V. Lamare, *J.F. Dozol, New J. Chem.* 20 (1996) 1183.
- [24] H.F. Ji, R. Dabestani, G.M. Brown, R.A. Sachleben, *Chem. Commun.* (2000) 833.
- [25] V. Souchon, I. Leray, B. Valeur, *Chem. Commun.* (2006) 4224.
- [26] H.M. Chawla, S.P. Singh, S. Upreti, *Tetrahedron* 62 (2006) 2901.
- [27] S. Garaudée, M. Elhabiri, D. Kalny, C. Robiollé, J.M. Trendel, R. Hueber, A.V. Dorselaer, P. Albrecht, A.M. Albrecht-Gary, *Chem. Commun.* 9 (2002) 944.
- [28] P. Kuad, R. Schurhammer, C. Maechling, C. Antheaume, C. Mioskowski, G. Wipff, B. Spiess, *Phys. Chem. Chem. Phys.* 11 (2009) 10299.
- [29] A. Le Roux, S. Meunier, T. Le Gall, J.M. Denis, P. Bischoff, A. Wagner, *Chem. Med. Chem.* 6 (2011) 561.
- [30] Y. Bourdreux, E. Bodio, C. Willis, C. Billaud, T. Legall, C. Mioskowski, *Tetrahedron* 64 (2008) 8930.
- [31] D. Habrant, A. Le Roux, S. Poigny, S. Meunier, A. Wagner, C. Mioskowski, *J. Org. Chem.* 73 (2008) 9490.
- [32] J. Volhard, *Justus Liebigs Ann. Chem.* 282 (1894) 1.
- [33] R.G. Bates, *Determination of pH – theory and practice*, Wiley-Interscience, New York, 1973.
- [34] R.A. Binstead, A.D. Zuberbühler, B. Jung, *SPECTFIT global analysis system version 3.04.34*, 2003.
- [35] R. Brouillard, *J. Chem. Soc., Faraday Trans. 1* (76) (1980) 583.
- [36] C.F. Bernasconi, *Relaxation Kinetics*, Academic Press, New York, 1976.
- [37] M. Eigen, L. DeMaeyer, *Techniques of Chemistry*, Wiley, New York, 1973.
- [38] J.M. El Hage Chahine, J.E. Dubois, *J. Am. Chem. Soc.* 105 (1983) 2335.
- [39] SYBYL, in: Tripos Inc., 1699 South Hanley Rd., St. Louis, MO 63144, USA.
- [40] D.A. Case, T.A. Darden, T.E. Cheatham, C.L. Simmerling, J. Wang, R.E. Duke, R. Luo, R.C. Walker, W. Zhang, K.M. Merz, B. Roberts, B. Wang, S. Hayik, A. Roitberg, G. Seabra, I. Kolossvary, K.F. Wong, F. Paesani, J. Vanicek, J. Liu, X. Wu, S. Brozell, T. Steinbrecher, H. Gohlke, Q. Cai, X. Ye, J. Wang, M.-J. Hsieh, G. Cui, D.R. Roe, D.H. Mathews, M.G. Seetin, C. Sagui, V. Babin, T. Luchko, S. Gusarov, A. Kovalenko, P.A. Kollman, *AMBER 11*, University of California, San Francisco, 2010.
- [41] J. Wang, R.M. Wolf, J.W. Caldwell, P.A. Kollman, D.A. Case, *J. Comput. Chem.* 25 (2004) 1157.
- [42] A. Jakalian, B.L. Bush, D.B. Jack, C.I. Bayly, *J. Comput. Chem.* 21 (2000) 132.
- [43] A. Jakalian, D.B. Jack, C.I. Bayly, *J. Comput. Chem.* 23 (2002) 1623.
- [44] J. Aqvist, *J. Phys. Chem.* 94 (1990) 8021.
- [45] C. Teixeira, N. Serradji, F. Maurel, F. Barbault, *Eur. J. Med. Chem.* 44 (2009) 3524.
- [46] W. Humphrey, A. Dalke, K. Schulten, *J. Mol. Graph.* 14 (1996) 33.
- [47] J.M. El Hage Chahine, A.M. Bauer, K. Baraldo, C. Lion, F. Ramiandrasoa, G. Kunesch, *Eur. J. Inorg. Chem.* (2001) 2287.
- [48] H.A. Benesi, J.H. Hildebrand, *J. Am. Chem. Soc.* 71 (1949) 2703.
- [49] P.B. Chock, *Proc. Natl. Acad. Sci. USA* 69 (1972) 1939.
- [50] F. Arnaud-Neu, Z. Asfari, B. Souley, J. Vicens, *New J. Chem.* 20 (1996) 453.
- [51] I. Leray, Z. Asfari, J. Vicens, B. Valeur, *J. Chem. Soc., Perkin Trans. 2* (2002) 1429.
- [52] P. Kuad, M. Borkovec, M. Desage-El Murr, T. Le Gall, C. Mioskowski, B. Spiess, *J. Am. Chem. Soc.* 127 (2005) 1323.
- [53] C. Chen, W. Wallace, E.M. Eyring, S. Petrucci, *J. Chem. Phys.* 88 (1984) 2541.
- [54] R.G. Pearson, *J. Am. Chem. Soc.* 110 (1988) 7684.
- [55] K. Lindorff-Larsen, P. Maragakis, S. Piana, M.P. Eastwood, R.O. Dror, D.E. Shaw, *PLoS One* 7 (2012) e32131.
- [56] K. Lindorff-Larsen, S. Piana, R.O. Dror, D.E. Shaw, *Science* 334 (2011) 517.
- [57] K. Lindorff-Larsen, N. Trbovic, P. Maragakis, S. Piana, D.E. Shaw, *J. Am. Chem. Soc.* 134 (2012) 3787.
- [58] D.E. Shaw, R.O. Dror, J.K. Salmon, J.P. Grossman, K.M. Mackenzie, J.A. Bank, C. Young, M.M. Deneroff, B. Batso, K.J. Bowers, E. Chow, M.P. Eastwood, D.J. Ieradi, J.L. Klepeis, J.S. Kuskin, R.H. Larson, K. Lindorff-Larsen, P. Maragakis, M.A. Moraes, S. Piana, Y. Shan, B. Towles, *Proceedings of the ACM/IEEE Conference on Supercomputing (SC09)* (2009) 1.
- [59] R. Schurhammer, R. Diss, B. Spiess, G. Wipff, *Phys. Chem. Chem. Phys.* 10 (2008) 495.
- [60] H.K. Frensdorff, *J. Am. Chem. Soc.* 93 (1971) 600.
- [61] V. Arora, H.M. Chawla, T. Francis, M. Nanda, S.P. Singh, *Ind. J. Chem.* 42A (2003) 3041.
- [62] V. Arora, H.M. Chawla, S.P. Singh, *Arkivoc* ii (2007) 172.
- [63] I. Leray, Z. Asfari, J. Vicens, B. Valeur, *J. Fluorescence* 14 (2004) 451.
- [64] T.C. Kim, S.S. Lee, J.S. Kim, *J. Kim, Anal. Sci.* 17 (2001) 573.